Tunable thermal rectification in graphene nanoribbons through defect engineering: A molecular dynamics study

Yan Wang, Siyu Chen, and Xiulin Ruan[a)]
School of Mechanical Engineering and the Birck Nanotechnology Center, Purdue University, West Lafayette, Indiana 47907, USA

(Received 29 January 2012; accepted 28 March 2012; published online 16 April 2012)

Using non-equilibrium molecular dynamics, we show that asymmetrically defected graphene nanoribbons (GNR) are promising thermal rectifiers. The optimum conditions for thermal rectification (TR) include low temperature, high temperature bias, ~1% concentration of single-vacancy or substitutional silicon defects, and a moderate partition of the pristine and defected regions. TR ratio of ~80% is found in a 14-nm long and 4-nm wide GNR at a temperature of 200 K and bias of 90 K, where heat conduction is in the ballistic regime since the bulk effective phonon mean-free-path is around 775 nm. As the GNR length increases towards the diffusive regime, the TR ratio decreases and eventually stabilizes at a length-independent value of about 3%–5%. This work extends defect engineering to 2D materials for achieving TR. © *2012 American Institute of Physics*. [http://dx.doi.org/10.1063/1.3703756]

Motivated by the important role that electronic diodes play in modern industry, many studies have been conducted in search of the thermal counterparts, i.e., thermal rectifiers, for applications in thermal management and thermal signal processing.[1–6] So far, most proposed or fabricated thermal rectifiers have asymmetric shape,[2–5] mass density,[1] or an interface between dissimilar materials.[7,8] However, the fabrication of such delicate structures[2,3,5] demands sophisticated patterning process which limits their stability.[9] The significant reduction of the effective thermal conductivity (κ) of thermal rectifiers utilizing interfaces[7,8] also limits the application of such design. A nano-device made of a single material, requiring minimum fabrication efforts and possessing high κ, is thus of great benefit to this field. Defect engineering is a promising approach in this regard. Thermal rectification (TR) in asymmetrically defected carbon nanotubes (CNT) has been reported in Refs. 10 and 11, where single-vacancy (SV) defect was considered and the TR was shown to be quite weak.[10]

Here we propose the pristine-defected graphene nanoribbon (pdGNR) as a promising thermal rectifier and systematically study the effects of design parameters. Graphene and graphene nanoribbon (GNR) have attracted extensive attention due to their outstanding thermal, electrical, mechanical, and optical properties.[2,12–15] Compared with other materials, the 2D nature of graphene and GNR allows for much easier artificial introduction of defects,[16] which is essential for tailoring the thermal and electrical properties of pristine materials for various applications including TR. As 2D GNRs have distinctly different thermal transport properties[17] from 1D CNTs, detailed analysis on TR in such systems is necessary and will facilitate the exploration of high-performance thermal rectifiers. Here we consider GNR with length ranging from 14 nm to 6 μm. Since the effective bulk phonon mean-free-path (MFP) in graphene is around 775 nm,[18] our GNR length covers both the ballistic and diffusive phonon transport regimes.

As shown in Fig. 1(a), SV and di-vacancy (DV) can be created by removing a single C atom or two neighboring atoms.[19] If a C–C bond is rotated by 90°, four hexagons in the graphene lattice are transformed into two pentagons and two heptagons, which forms the Stone-Wales defect [SW(55–77)].[16,19] These types of point defects were found to reduce the κ of pristine GNRs significantly (> 65%) with a concentration of one defect per thousand atoms.[20] Substitutional silicon defect (Si) was also predicted to be stable in GNRs and correlated with a drastic reduction of κ in a first-principles study.[21] In our work, defects are created randomly, based on a prescribed concentration (α), in the right side of the GNR, as indicated by the dashed line in Fig. 1(b). α is defined as the ratio of the number of defected nodes to the total number of the nodes in the right side of the hexagon network. Non-equilibrium molecular dynamics (MD) is performed using LAMMPS.[22] Periodic boundary condition is applied to the width (Y) direction to eliminate the edge effects, as the dangling edges are also defects (extended

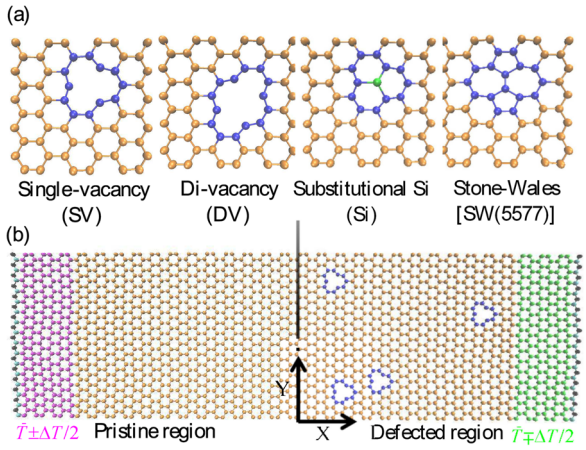

FIG. 1. (a) Types of point defect studied in this work. (b) Simulation domain setup for pdGNRs. The dashed line divides the GNR into pristine region and defected region, where defects are randomly created inside the latter.

[a)]Electronic mail: ruan@purdue.edu.

defect) in a broad sense.[20] We have checked that the width has minor effect on simulation results for GNRs wider than 3.3 nm, and hence the 4.0 nm wide GNRs used here suffer negligible size effects in the Y direction. The outermost columns of atoms at the two ends of the GNR in the length (X) direction are fixed to avoid the sublimation of atoms, and free boundary condition is applied to the cross-plane direction. The C-Si and C-C interactions are modeled with the original[23] and the optimized[24] Tersoff potential, respectively. The optimized Tersoff is adopted here due to its improved description of the anharmonicity and acoustic-phonon dispersions compared to other available potentials,[24] which are important to thermal transport. The GNR is first relaxed at zero pressure and constant temperature, $\bar{T}$, for 3×10^6 time steps (0.25 fs per step) using the Nosé-Hoover thermostat.[25,26] Then, two different temperatures, i.e., $\bar{T} + \Delta T/2$ and $\bar{T} - \Delta T/2$, are applied to regions adjacent to the ends of the GNR using two Nosé-Hoover thermostats, and steady state is achieved after 0.5 ns. The simulation is then continued for another 2 ns for data collection. The heat current resulting from the temperature bias, ΔT, is computed as $J = \left(\frac{dE_{hot}}{dt} + \frac{dE_{cold}}{dt}\right)/2$, where E_{hot} and E_{cold} are the total energy that has been added to or subtracted from the atoms in the hot and cold thermostats, respectively. To quantify TR in a common manner,[1–6] we designate

$$\eta = \frac{J_+ - J_-}{J_-} \tag{1}$$

as the TR ratio, where J_+ is the heat current when the thermostat in the pristine side is maintained at $\bar{T} + \Delta T/2$ and that in the defected side is maintained at $\bar{T} - \Delta T/2$ and vice versa for J_-.

We herein study the effect of $\bar{T}, \Delta T, \alpha$, type of defect, length of the GNR, and the ratio of the length of the pristine region to that of the defected region ($R_L = L_{pristine}/L_{defected}$), thus covering most of the factors that may affect thermal properties of defected GNRs greatly. To account for the randomness of defects, twelve independent simulations are run on independently generated GNRs with random defects for each data point.

First, we evaluate η in GNRs composed of a 7 nm long pristine region and a 7 nm long defected region. GNRs with four types of defect, i.e., SV, DV, Si, and SW(55–77), are studied in separate simulations with $\alpha = 1.5\%$. We vary the average temperature $\bar{T}$ and use $\Delta T = 90$ K for all cases. As shown in Fig. 2, TR is significant ($\eta \approx 0.7$ for SV and Si and $\eta \approx 0.3$ for DV and SW(55–77)) at 200 K, but weakens at higher temperatures). Similar trend was also found in other types of thermal rectifiers[2,3,6,9,27] and is usually attributed to the mismatch of the phonon spectra between the two sides of a rectifier. When the average temperature increases, such difference becomes weaker with respect to the total vibrational energy, and hence TR is suppressed. Comparing η of different types of defect at the same $\bar{T}$, we find GNRs with SV and Si defects rectify heat flow more strongly than those with DV and SW(55–77) defects. Note that each DV or SW(55–77) defect contributes two defected nodes to the carbon network of graphene, i.e., two defected nodes per defect. Accordingly, with the same α (same number of defected nodes), SV and Si defects are more scattered than DV and SW(55–77), and hence the formers tune the phonon transport more strongly than the latters. Reference 20 revealed that with $\alpha = 0.1\%$, SV defects reduce the κ of GNRs by 81%, while DV and SW(55–77) only reduce it by 61%, in consistency with our work.

We plot the η of pdGNRs as a function of the MFP normalized length (L/MFP) for different ΔT in Fig. 3(a) and find that $|\eta|$ increases as ΔT increases, consistent with previous studies.[28,29] Notably, $|\eta|$ decreases as the GNR length increases up to 100 nm as predicted by MD, indicating that this type of thermal rectifier has the best rectifying power at small size. This observation inspires us to check whether TR should diminish at macroscopic size. Here we consider ($L \geq 2$ μm) where heat conduction transits to the diffusive regime, and we use the conventional Fourier equation to evaluate TR. We fit the κ of pristine and defected GNRs (Ref. 20) as a function of temperature and numerically solve the 1D, steady-state heat conduction equation $\nabla_x\{\kappa[x, T(x)]\nabla_x T\} = 0$ with the temperature at the two ends maintained at 300 K $+ \Delta T/2$ and 300 K $- \Delta T/2$, respectively. In this regime, pdGNRs show a length-independent TR of 3%–5% for the different ΔT considered here. The TR

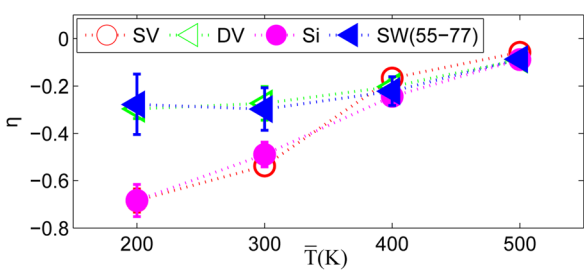

FIG. 2. Temperature dependence of η for pdGNRs with different types of point defect.

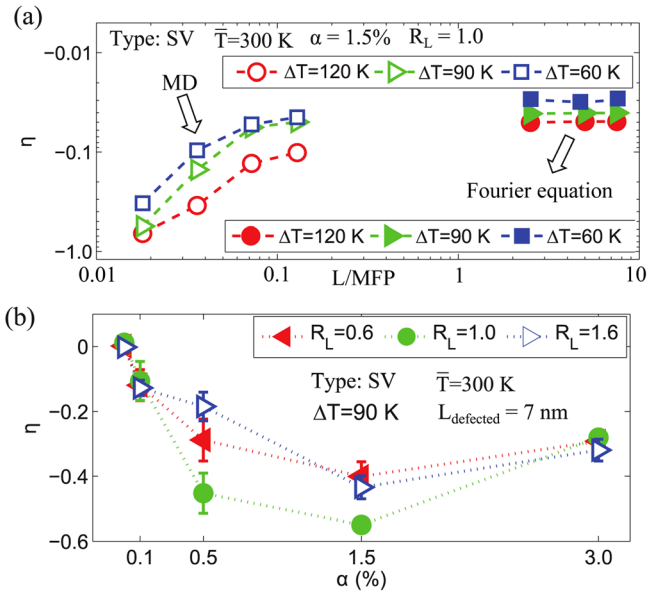

FIG. 3. (a) η as a function of L/MFP of the pdGNRs for different ΔT, where MFP = 775 nm is used. Data points denoted by unfilled and filled markers are computed by MD simulation and by solving the 1D, steady-state Fourier heat conduction equation, respectively. (b) η as a function of α for pdGNRs with different R_L.

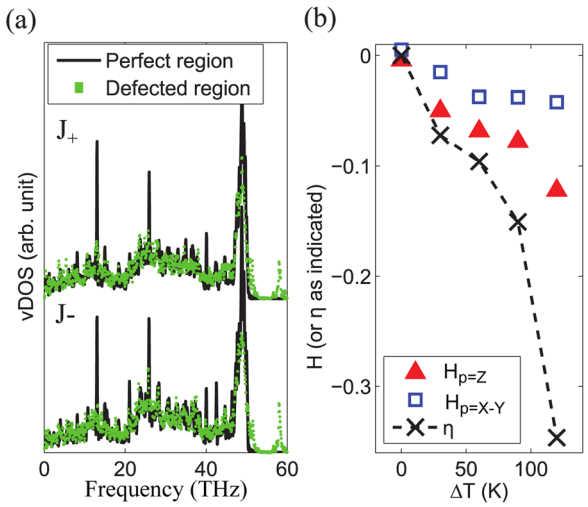

FIG. 4. (a) vDOS of the perfect region and defected region for opposite heat flow directions. (b) H and η for various ΔT.

mechanism becomes the same as the bulk thermal rectifier proposed in Ref. 7, i.e., the $\kappa(x,T)$ is not a separable function of x and T. This non-diminishing, length-independent TR in macroscopic defected GNR is distinct from that of rectifiers using asymmetric shapes,[2–4] which completely lose TR at macroscopic length.[30]

We then consider the effect of R_L: $R_L \to \infty$ means a pristine GNR, while $R_L \to 0$ means a homogeneously defected GNR. Both extremes reduce to a symmetric structure and thus cannot rectify heat flow. Figure 3(b) shows that a moderate partition ($R_L \approx 1.0$) of the pristine and defected region usually generates higher $|\eta|$ than biased cases. Similarly, a medium α ($0.5\% \sim 1.5\%$) is also preferable to the extremes since very low α corresponds to pristine GNR and very high α reduces κ too much for both directions. Thus, as for defect engineering, we conclude that an α on the order of 1% is needed for TR, compared with 0.1% for notably reducing κ and 0.0001% for tailoring electronic properties.[16]

Figure 4 shows the vibrational density of states (vDOS), which is the summation of the Fourier transform of the autocorrelation function of atomic velocities in each polarization ($p = $ X, Y, Z).[28] For both forward (J_+) and reversed (J_-) heat flow, we calculate the overlap (S) between the acoustic region[24] of the vDOS of the pristine and defected region using the method in Ref. 28. In parallel with Eq. (1), we compute $H = (S_+ - S_-)/S_-$ for both in-plane (X-Y) and out-of-plane (Z) polarizations to show the change of S when the sign of ΔT reverses. Consistent with previous studies,[10,11,28] η and H have the same sign and show quite strong positive correlation, which confirms the suitability of the spectra overlap theory[28] as a qualitative explanation to TR.

As a final remark, note that in contrast to other GNR-based thermal rectifiers[2,3] of asymmetric shape that induces asymmetric boundary scattering of phonons,[1] the asymmetrically defected GNRs proposed here favor large width, thus saving the need for complicated patterning process in making the narrow and regular shapes. For very narrow GNRs, there is very high concentration of *edge* defects,[20] and they dominate the thermal transport instead of the asymmetrically introduced point defects, and hence TR is greatly reduced.

In summary, we studied the TR effect in asymmetrically defected GNRs using classical MD simulations. Low $\bar{T}$, high ΔT, moderate α ($\sim$1%) and R_L, and short system length were found to be optimum for high thermal rectifying efficiency of the thermal rectifier proposed in this work. We also revealed that SV and Si defects tune thermal transport more strongly than DV and SW(55–77) defects with the same concentration and are thus preferable in making thermal rectifiers. The TR decreases as the GNR length increases and eventually stabilizes at a length-independent value for macroscopic length when heat conduction transits to the diffusive regime. This work extends defect engineering to the field of thermal management and thermal signal manipulation with 2D thermal rectifiers.

The authors thank the support from the Air Force Office of Scientific Research (AFOSR) and the Cooling Technologies Research Center, an NSF Industry & University Cooperative Research Center. The authors also acknowledge the helpful suggestions from Hua Bao to this work.

[1]C. W. Chang, D. Okawa, A. Majumdar, and A. Zettl, Science **314**, 1121 (2006).
[2]J. Hu, X. Ruan, and Y. P. Chen, Nano Lett. **9**, 2730 (2009).
[3]N. Yang, G. Zhang, and B. Li, Appl. Phys. Lett. **95**, 033107 (2009).
[4]J. Hu, Y. Wang, A. Vallabhaneni, X. Ruan, and Y. P. Chen, Appl. Phys. Lett. **99**, 113101 (2011).
[5]N. A. Roberts and D. G. Walker, ASME Conf. Proc. **2011**, T30053.
[6]M. Alaghemandi, F. Leroy, F. Müller-Plathe, and M. C. Böhm, Phys. Rev. B **81**, 125410 (2010).
[7]D. Sawaki, W. Kobayashi, Y. Moritomo, and I. Terasaki, Appl. Phys. Lett. **98**, 081915 (2011).
[8]M. Hu, J. V. Goicochea, B. Michel, and D. Poulikakos, Appl. Phys. Lett. **95**, 151903 (2009).
[9]W.-R. Zhong, W.-H. Huang, X.-R. Deng, and B.-Q. Ai, Appl. Phys. Lett. **99**, 193104 (2011).
[10]K. Takahashi, M. Inoue, and Y. Ito, Jpn. J. Appl. Phys. **49**, 02BD12 (2010).
[11]H. Hayashi, Y. Ito, and K. Takahashi, J. Mech. Sci. Technol. **25**, 27 (2011).
[12]A. A. Balandin, Nat. Mater. **10**, 569 (2011).
[13]D. L. Nika, E. P. Pokatilov, A. S. Askerov, and A. A. Balandin, Phys. Rev. B **79**, 155413 (2009).
[14]A. K. Geim, Science **324**, 1530 (2009).
[15]A. Vakil and N. Engheta, Science **332**, 1291 (2011).
[16]L. D. Carr and M. T. Lusk, Nat. Nano **5**, 316 (2010).
[17]L. Lindsay, D. A. Broido, and N. Mingo, Phys. Rev. B **82**, 161402 (2010).
[18]S. Ghosh, I. Calizo, D. Teweldebrhan, E. P. Pokatilov, D. L. Nika, A. A. Balandin, W. Bao, F. Miao, and C. N. Lau, Appl. Phys. Lett. **92**, 151911 (2008).
[19]F. Banhart, J. Kotakoski, and A. V. Krasheninnikov, ACS Nano **5**, 26 (2011).
[20]J. Haskins, A. Kinaci, C. Sevik, H. Sevincli, G. Cuniberti, and T. Cagin, ACS Nano **5**, 3779 (2011).
[21]J.-W. Jiang, B.-S. Wang, and J.-S. Wang, Appl. Phys. Lett. **98**, 113114 (2011).
[22]S. Plimpton, J. Comput. Phys. **117**, 1 (1995).
[23]J. Tersoff, Phys. Rev. B **37**, 6991 (1988).
[24]L. Lindsay and D. A. Broido, Phys. Rev. B **81**, 205441 (2010).
[25]S. Nose, J. Chem. Phys. **81**, 511 (1984).
[26]W. G. Hoover, Phys. Rev. A **31**, 1695 (1985).
[27]N. Yang, G. Zhang, and B. Li, Appl. Phys. Lett. **93**, 243111 (2008).
[28]J. Lan and B. Li, Phys. Rev. B **74**, 214305 (2006).
[29]B. Hu and L. Yang, Chaos: Interdiscip. J. Nonlinear Sci. **15**, 015119 (2005).
[30]Y. Wang, A. Vallabhaneni, J. Hu, B. Qiu, Y. P. Chen, and X. Ruan, "Thermal rectification in asymmetric nanostructures of a single material," (unpublished).